Article (refereed) - postprint

Starnes, Daniel; Unrine, Jason; Chen, Chun; Lichtenberg, Stuart; Starnes, Catherine; Svendsen, Claus; Kille, Peter; Morgan, John; Baddar, Zeinah Elhaj; Spear, Amanda; Bertsch, Paul; Chen, Kuey Chu; Tsyusko, Olga. 2019. **Toxicogenomic responses of Caenorhabditis elegans to pristine and transformed zinc oxide nanoparticles**. *Environmental Pollution*, 247. 917-926. https://doi.org/10.1016/j.envpol.2019.01.077

# Toxicogenomic responses of *Caenorhabditis elegans* to pristine and transformed Zinc Oxide nanoparticles

**Daniel Starnes[1,2], Jason Unrine[1], Chun Chen[1,3], Stuart Lichtenberg[1], Catherine Starnes[2,4] Claus Svendsen[5], Peter Kille[6], John Morgan[6], Zeinah Elhaj Baddar[1], Amanda Spear[7], Paul Bertsch[8], Kuey Chu Chen[9], and Olga Tsyusko[1,*]**

1. Department of Plant and Soil Sciences, University of Kentucky, Lexington, Kentucky, USA
2. Department of Math and Computer Science, Belmont University Nashville TN, USA
3. State Key Laboratory of Crop Stress Biology in Arid Areas, College of Life Sciences, Northwest A&F University, Yangling Shaanxi 712100, P. R. China
4. Biostatics, Epidemiology, and Research Design; Center for Clinical and Translational Science ,University of Kentucky, Lexington KY, USA
5. Centre for Ecology and Hydrology, Maclean Building, Benson Lane, Crowmarsh Gifford, Wallingford, Oxon OX10 8BB, UK
6. Organisms and Environment Division, Cardiff School of Biosciences, Cardiff University, Cardiff, CF10 3AT, UK
7. Department of Toxicology and Cancer Biology, University of Kentucky, Lexington, KY, USA
8. Division of Land and Water, CSIRO, Ecosciences Precinct, Brisbane, QLD Australia
9. Department of Pharmacology and Nutritional Sciences, College of Medicine, University of Kentucky, Lexington, KY, USA

*Corresponding author: olga.tsyusko@uky.edu, University of Kentucky, 1100 S. Limestone St., Agriculture Science Center North, Lexington, KY 40546; phone 859-257-1777

## Abstract

Manufactured nanoparticles (MNPs) undergo transformation immediately after they enter wastewater treatment streams and during their partitioning to sewage sludge, which is applied to agricultural soils in form of biosolids in many parts of the world. We examined toxicogenomic responses of the model nematode *Caenorhabditis elegans* to pristine and transformed ZnO-MNPs (phosphatized pZnO- and sulfidized sZnO-MNPs). To account for the toxicity due to dissolved Zn, a $ZnSO_4$ treatment was included. Transformation of ZnO-MNPs reduced their toxicity by nearly ten-fold, while there was almost no difference in the toxicity of pristine ZnO-MNPs and $ZnSO_4$. This combined with the fact that far more dissolved Zn was released from ZnO- compared to pZnO- or sZnO-MNPs, suggests that dissolution of pristine ZnO-MNPs is one of the main drivers of their toxicity. Transcriptomic responses at the $EC_{30}$ for reproduction resulted in a total of 1161 differentially expressed genes. Fifty percent of the genes differentially expressed in the $ZnSO_4$ treatment, including the three metal responsive genes (*mtl-1*, *mtl-2* and *numr-1*), were shared among all treatments, suggesting that responses to all forms of Zn could be partially attributed to dissolved Zn. However, the toxicity and transcriptomic responses in all MNP treatments cannot be fully explained by dissolved Zn. Two of the biological pathways identified, one essential for protein biosynthesis (Aminoacyl-tRNA biosynthesis) and another associated with detoxification (ABC transporters), were shared among pristine and one or both transformed ZnO-MNPs, but not $ZnSO_4$. When comparing pristine and transformed ZnO-MNPs, 66% and 40% of genes were shared between ZnO-MNPs and sZnO-MNPs or pZnO-MNPs, respectively. This suggests greater similarity in transcriptomic responses between ZnO-MNPs and sZnO-MNPs, while toxicity mechanisms are more distinct for pZnO-MNPs, where 13 unique biological

pathways were identified. Based on these pathways, the toxicity of pZnO-MNPs is likely to be associated with their adverse effect on digestion and metabolism.

**Keywords:** gene expression, nanomaterial, nematode, transcriptomics, soil, wastewater

## Capsule

The toxicity and transcriptomics responses of transformed ZnO nanoparticles are distinct from pristine ZnO nanoparticles and only partially due to release of ions.

## Introduction

The growth of the nanotechnology industry continues rapidly, as indicated by increases in both the number of products containing nanomaterials and the variety of manufactured nanoparticles (MNPs) reaching the market (Vance, Kuiken et al. 2015). Many products containing MNPs are incorporated into consumer products prior to full consideration of their potential environmental implications. Zinc oxide MNPs (ZnO-MNPs) possess unique physico-chemical properties that allow for a wide array of applications, from biosensors, to optical devices, to personal care products(Zhong Lin 2004). Recent estimates for global production of ZnO-MNPs exceeds 550 tons annually with nearly all of those MNPs being used in cosmetics, sunscreens, and paints (Spisni, Seo et al. 2016). With increased ZnO-MNPs use in consumer products, the primary pathway by which ZnO-MNPs enter the environment is through the land application of biosolids from wastewater treatment plants (WWTP) (Ju-Nam and Lead 2008, Mueller and Nowack 2008). After entering the wastewaters, MNPs partition to sewage sludge (Ma, Levard et al. 2014), the majority of which is land applied as a soil amendment. For example, yearly 60% (US), 70% (United Kingdom), and 80% (Spain) of all biosolids from WWTPs are applied to land (EPA 1995, Mueller and Nowack 2008, Gottschalk, Sonderer et al. 2009, Lucid, Fenton et al. 2013). Given that wastewater and sewage sludge are enriched in $SH^-$ and $PO_4$-$^{3-}$, two of the primary transformation processes for ZnO-MPNs, phosphatation and sulfidation, will result in formation of $Zn_3(PO_4)_2$ and ZnS containing solid phases (Martínez, Bazilevskaya et al. 2006, Lombi, Donner et al. 2012, Ma, Levard et al. 2014).

Pristine, which we define as “as synthesized”, ZnO-MNPs have already been shown to cause toxicity in *C. elegans* by negatively impacting their growth, reproduction, and increasing their mortality (Gupta, Kushwah et al. 2015). In the same study, using fluorescently labeled ZnO-

MNPs, the authors showed that the MNPs were deposited in the intestinal tissues of the nematodes. ZnO-MNPs have been found to have a wide concentration range for mortality to *C. elegans*, from 2.2 mg $L^{-1}$ up to the 780 mg $L^{-1}$, depending on the exposure media (Ma, Bertsch et al. 2009, Wang, Wick et al. 2009). Using *Danio rerio* (zebrafish), Xiaoshan et al. showed that ZnO-MNPs were more effective at generating reactive oxygen species in embryos compared to dissolved Zn when exposed to equal concentrations on a Zn basis(Xiaoshan, Jiangxin et al. 2009). ZnO-MNPs have been shown to induce oxidative stress response genes in *C. elegans*(Gupta, Kushwah et al. 2015), *Eisenia fetida(Mwaanga P. 2017)*, *Arabidopsis thaliana* (Landa, Vankova et al. 2012), and *Danio rerio* (Xiaoshan, Jiangxin et al. 2009).

The majority of the research conducted on the toxicity of ZnO-MNPs has utilized mostly commercially available pristine ZnO-MNPs, while information on the effects of transformedZnO-MNPs is limited. The study which examined effects of ZnO-MNPs, aged in different soils for 56 and 142 days, to *Eisenia andrei* demonstrated that weight was the only variable affected by the aging of ZnO-MNPs. The aging of ZnO-MNPs did not affect earthworms' reproduction (Romero-Freire, Lofts et al. 2017). Among studies on the effects of transformed (simulated "aging") metal nanomaterials in invertebrates, more emphasis has been given to sulfidized Ag-MNPs, which are the primary transformation products of Ag-MNPs in wastewater, sewage sludge and biosolids. Sulfidized sAg-MNPs showed significant decreases in Ag bioavailability and their toxicity in *C. elegans* as well as different toxicity mechanisms when compared to pristine Ag-MNPs (Levard, Hotze et al. 2013, Starnes, Unrine et al. 2015, Starnes D. 2016). When a model legume *Medicago truncatula* was grown in soils-amended with biosolids containing a mixture of transformed Ag-, ZnO- and $TiO_2$-MNPs, exposure adversely affected the plant's nodulation rate and caused plant toxicity. The transcriptomic data combined with the metal uptake data suggested that the observed

effects were likely due to increased bioavailability of Zn from ZnO-MNPs and were more pronounced for transformed MNPs than for transformed bulk metals (Chen, Unrine et al. 2015, Judy, McNear et al. 2015). When testing the same biosolids amended soils in *E. fetida*, it was also found that the biosolids containing transformed MNPs were more toxic to reproduction than the biosolids containing transformed bulk metals (Lahive, Matzke et al. 2017). To our knowledge, there are no studies that have investigated the toxicogenomic effects of pristine ZnO-MNPs as compared to phosphatized- and sulfidized ZnO-MNPs. Given that both transformed forms of ZnO-MNP are predicted to be present in biosolids applied to agricultural fields, this represents a gap in the understanding of the risks that ZnO-MNPs possess to environmental health.

The purpose of this study was to investigate and compare the toxicity and transcriptomic responses of *C. elegans* exposed to pristine ZnO-MNPs and transformed phosphatized and -sulfidized, ZnO-MNPs and $ZnSO_4$. Our hypothesis is that the mode of toxicity would differ between pristine and transformed ZnO-MNPs, and that those would be distinct from the response to $ZnSO_4$ exposure. Due to the high solubility of ZnO-MNPs, we also hypothesized that significant part of the response of *C. elegans* to pristine ZnO MNPs would be due to the dissolved Zn

## Materials and Methods

*Zinc Oxide Nanoparticle Synthesis and Characterization*

Protocols for ZnO-MNPs synthesis and characterization were adapted from previously published research from our laboratory (Ma, Levard et al. 2013, Rathnayake, Unrine et al. 2014). Pristine and transformed ZnO-MNPs started with the dispersion of uncoated ZnO (Nanosun, Micronisers, Melbourne, Victoria, Australia) with a nominal primary particle size of 30 nm. Primary particle size distribution for both pristine and transformed ZnO-MNPs was determined using transmission electron microscopy (TEM; JEOL 2010F, Tokyo, Japan); 10 μL of 200 mg

Zn $L^{-1}$ ZnO-MNPs were placed on formvar coated 200 mesh Cu grids and allowed to air dry in a laminar flow hood, 100 particles were measured from three separate micrographs. The exposure solutions with pH of 8.2 were prepared in synthetic soil pore water (SSPW) and were used to determine electrophoretic mobility and hydrodynamic diameter of ZnO-MNPs. The mean intensity weighted (z-average) hydrodynamic diameters were measured in exposure media (SSPW) at 100 mg Zn $L^{-1}$ using dynamic light scattering (DLS, Malvern ZetaSizer Nano-ZS, Malvern, United Kingdom). Zeta potentials (ZP) of both pristine and transformed ZnO were calculated using the Hückel approximation in SSPW using 100 mg Zn $L^{-1}$ suspensions from electrophoretic mobilities measured by phase analysis light scattering (PALS, Malvern Zetasizer Nano-ZS). The Z-average (intensity weighted) diameter of the pristine ZnO-MNPs in the exposure media was 265 nm.

*Transformation of pristine ZnO-MNPs*

Phosphatized ZnO-MNPs were generated by dispersing 25 mg Zn $L^{-1}$ of nanoSun ZnO powder into 50 ml of 5.3 mM solution of (pH adjusted to 6) in polypropylene centrifuge tubes. The concentration of $Na_2HPO_4$ used for the phosphatation has been predicted to result in complete transformation of ZnO-MNPs in wastewater (Rathnayake, Unrine et al. 2014). Ten replicates were created and each tube was sealed with parafilm and placed horizontally in racks on a reciprocating shaker for 5 days according to Rathnayake et al., 2014 (Rathnayake, Unrine et al. 2014). . Following incubation, the tubes were centrifuged at 3320 x g for 20 min. Supernatants were decanted and pellet was resuspended in ultra-pure 18 MΩ water. This process was repeated three times to ensure that all residual $Na_2HPO_4$ was removed. Sulfidized ZnO-MNPs were prepared at a concentration of 42 mg Zn $L^{-1}$ by dispersing nanoSun powder into 50 ml of 0.06 M solution of $Na_2S$ in He-sparged water in polypropylene centrifuge tubes. According to Ma et al. study (Ma,

Levard et al. 2013), use of this $Na_2S$ concentration is expected to result in complete sulfidation of ZnO-MNPs. Ten replicates were created and each was filled to maximum capacity to minimize the headspace in the tube. Tubes were sealed with a double layer of parafilm and placed horizontally in racks on a reciprocating shaker for 5 d. Following incubation tubes were centrifuged at 5000 x g for 1 h. Supernatants were decanted and the pellet was re-suspended in ultra-pure water. This process was repeated 3 times to ensure that all residual $Na_2S$ was removed. After final wash, transformed nanoparticles were lyophilized and transformation was confirmed by comparing to authentic standards using powder X-ray diffraction (PANalytical x'pert Pro). Stock solutions of the transformed and pristine MNPs were dispersed in ultra-pure water at 100 mg Zn $L^{-1}$ with continuous sonication in a water cooled-cup-horn sonicator for 45 min at 100% power (Misonix, Newtown CT, USA). TEM images, energy dispersive spectroscopy (EDS) and DLS particle size distributions, including DLS data in actual exposure media, hydrodynamic diameter (volume weighted) and zeta potential are given in Supporting Information (Table S1, Figures S1- S4). The Z-average (intensity-weighted) diameters of pZnO-MNPs and sZnO-MNPs in the exposure media (SSPW) were 1715 nm and 1022 nm, respectively. Powder X-ray fractograms and X-ray diffraction patterns (XRD) for pristine and phosphatized ZnO nanoparticles are presented in Figs. S5 and S6.

*Nematode exposures and toxicity experiments*

All exposures were conducted in SSPW (Na 4 mM, Mg 0.5 mM, Al 1 μM, K 1.0 mM, Ca 1.25 mM, $NO_3$ 3.5 mM, $SO_4$ 0.5 mM, $PO_4$ 1.0 μM, and $I$=10.3 mM). A complete description of SSPW can be found in Tyne et al. (Tyne, Lofts et al. 2013); however, we modified our solutions by omitting the iron to avoid the formation of Fe-oxohydroxide solids, which may form heteroaggregates with the MNPs, complicating our ability to characterize the exposure solutions

and interpret the results. We also omitted fulvic acid to further isolate the transformation effects of phosphate and sulfide on ZnO-MNP toxicity (Tyne, Lofts et al. 2013). The solutions were aerated overnight and the pH adjusted to 8.2 with 0.1 M NaOH (Tyne, Lofts et al. 2013).

The toxicity protocols represent modifications of previously established *C. elegans* toxicity testing methods (Tsyusko, Unrine et al. 2012, Starnes, Unrine et al. 2015). Wild type N2 Bristol strain of *C. elegans* were obtained from the Caenorhabditis Genetics Center (CGC) and were age-synchronized using NaClO/NaOH solution (Williams and Dusenbery 1988). For mortality testing, larval L3 stage nematodes were exposed to varying concentrations of $ZnSO_4$, ZnO-, pZnO-, and sZnO-MNPs in SSPW without bacterial food for 24 h in a 24 well polycarbonate tissue culture plate. Four concentrations were used for every treatment. Unfed nematodes were exposed to $ZnSO_4$ (5-20 mg Zn $L^{-1}$), ZnO-MNPs (5-20 mg Zn $L^{-1}$), pZnO-MNPs (50-200 mg Zn $L^{-1}$) and sZnO-MNPs (50-200 mg Zn $L^{-1}$). Exposures without feeding were conducted to differentiate between mortality due to dissolution and mortality due to intact particles, where dissolution and subsequent binding of $Zn^{2+}$ ions to microbial cells would have complicated our ability to quantify exposure to $Zn^{2+}$ ions (Levard, Yang et al. 2014). Each treatment had four replicates per concentration with 10 (±1) nematodes in each well and all concentrations were tested in two independent experiments.

For reproduction, eggs were hatched on K-agar plates with OP50 bacterial lawns (Williams and Dusenbery 1988) and were placed into the exposure solutions. For each exposure, six L1 nematodes were exposed to four concentrations per treatment of $ZnSO_4$ (0.5-2.0 mg Zn $L^{-1}$), ZnO-MNPs (0.5-2.0 mg Zn $L^{-1}$), pZnO-MNPs (5.0-20.0 mg Zn $L^{-1}$) and sZnO-MNPs (5.0-20.0 mg Zn $L^{-1}$) in SSPW. These concentrations were chosen to avoid mortality >10%. Reproduction experiments were conducted in the presence of bacterial food, *E. coli* (OP50 strain), added ($OD_{600}$

= 1) at the rate of 10 μL $mL^{-1}$ of exposure solution. Exposure solutions for reproduction experiments were replaced after 24 h and fresh bacterial food was added. After 50 h of exposure, individual nematodes were transferred to K-agar plates for egg laying. Adult worms were transferred to fresh K-Agar plates every 24 h for 72 h. Plates were incubated for 24 h to allow hatching, then stained with Rose Bengal (0.5 mg $L^{-1}$), heated to 50°C for 55 min, then fully hatched juveniles were counted. Each exposure was tested in two independent experiments. $EC_{30}$ values were calculated from parameters determined using linear regression.

To help quantify effects of dissolved Zn when exposed to ZnO-, pZn- or sZnO-MNP treatments, particle free supernatants were generated by centrifuging suspension of ZnO-MNPs in SSPW at 16,800 x g in for 3 hours after 24 hour incubation at 20°C. Immediately after centrifugation, the supernatant was decanted and used for the exposures. Nematodes exposed to particle free supernatants were compared to nematodes exposed to whole suspensions that had been incubated for 24 h. The highest concentration was selected for all treatments, and the exposure conditions were the same as in the experiments for mortality tests ($ZnSO_4$ and ZnO-MNPs 20 mg $L^{-1}$, pZnO-MNPs and sZnO-MNPs 200 mg $L^{-1}$).

*Nematode exposure and microarrays*

Nematodes at L1 stage were exposed at sublethal equitoxic concentrations (the $EC_{30}$ for reproduction) to $ZnSO_4$ (0.75 mg Zn $L^{-1}$), ZnO-MNPs (0.75 mg Zn $L^{-1}$), pZnO-MNPs (7.5 mg Zn $L^{-1}$) and sZnO-MNPs (7.5 mg Zn $L^{-1}$) for 48 hours. All exposures for microarrays were conducted in the presence of bacterial food, *E. coli* (OP50 strain), at the rate of 10 μL stock solution per mL of exposure solution ($OD_{600}$ = 1 for stock solution). To ensure a consistent exposure over the course of 48 hours, exposure solutions were replaced after 24 h with fresh ones and fresh bacterial food was added. Exposures were carried out in 15 mL polypropylene centrifuge tubes containing 4 mL

of exposure solution. The tubes were arranged horizontally in an incubator and three replicates per treatment were prepared. After exposure, RNA was extracted from each replicate using Trizol with subsequent purification with Qiagen RNeasy Kit (Qiagen, Chatsworth, CA). Cells were lysed using multiple freeze-thaw cycles (-80 and 37 °C) as previously described (Tsyusko, Unrine et al. 2012). All samples were checked for RNA integrity using a Nanodrop ND-2000 spectrophotometer and Agilent 2100 Bioanalyzer to examine the quality and quantity of the RNA samples. All RNA samples had RNA integrity numbers of nine and above and were sent to the Microarray Core Facility at the University of Kentucky to be processed for RNA transcriptome assay using Affymetrix *C. elegans* whole genome whole transcriptome (WT) microarrays. A total of 100 ng of total RNA was used to generate labeled ss-cDNA using Affymetrix WT Plus kit. The labeled ss-cDNA (5.0 µg) were fragmented and hybridized to EleGene 1.0 ST arrays for 16 h at 45°C in a hybridization oven with rotation at 60 RPM. The arrays were washed and stained using the Affymetrix 450 fluidics station and scanned on the Affymetrix GeneChip 7G scanner.

*Microarray data analysis*

Raw data signal intensity files were normalized using the robust multi-array average (RMA) algorithm following quantile normalization implemented in the Expression console (Affymetrix) in Partek Genomics Suite 7.0 (Partek, Inc., St. Louis, MO) (Irizarry, Hobbs et al. 2003). Microarray data were analyzed for differences between each treatment (ZnO-, pZnO-, sZnO-MNPs and ZnSO4) and control using one-way ANOVA with contrasts. The ANOVA data were filtered by unadjusted p-value of 0.05 in at least one of the treatments versus control. Multiple comparison correction function FDR step-up in Partek was applied to calculate the false discovery rate (FDR) for each experimental condition for every differentially expressed gene. After that the threshold was set at fold change (FC) ±2 with FDR < 0.2 to balance the protection against false

245 positives while minimizing the rate of false negatives. In Partek, all genes that were significantly
246 different from control in at least one treatment were analyzed using agglomerative hierarchical
247 cluster analysis (HCA). HCA is a 2-Pass clustering method; the first pass is a K-means clustering
248 and in the second pass the K-means clusters are joined by agglomerative clustering. The final lists
249 of differentially expressed genes that were significantly different from control in each treatment
250 were then used for pathway analysis using the Kyoto Encyclopedia of Genes and Genomes
251 (KEGG) search tools, integrated in Partek, to investigate the possible involvement of relevant
252 pathways. The same gene lists were also used with the functional annotation clustering tool in
253 bioinformatics resource DAVID 6.8(Huang da, Sherman et al. 2009, Huang da, Sherman et al.
254 2009) to identify significant changes within each of the gene lists for the enriched biological
255 pathways. We have also applied Pathview Web (Luo, Pant et al. 2017), which is an user friendly
256 open source for the pathway visualization and data integration, to screen for biological pathways
257 using the same gene lists. The gene ontology analysis functionality was utilized in Partek to screen
258 terms for biological processes (BP), molecular function (MF), and cellular compartment (CC)
259 using default settings. All microarray data have been submitted (Accession # GSE114881) to the
260 National Center for Biotechnology Information (NCBI).

261 *qRT-PCR.*

262 Quantitative reverse transcription polymerase chain reaction (qRT-PCR) analyses were
263 performed on samples in triplicates (both biological and technical) from independent experiment.
264 Y45F10D.4 was selected as the reference gene, which had no significant changes across treatments
265 in either microarray or qRT-PCR analysis. Y45F10D.4 encodes for a putative iron-sulfur cluster
266 enzyme has been shown to be an excellent candidate for use as reference gene in nanotoxicity
267 (Xiu, Zhang et al. 2012). Four differentially expressed genes were selected for qRT-PCR

confirmation. Among them were p-glycoproteins (*pgp-5 and pgp-6*), nuclear localized metal responsive (*numr-1*), and scramblase (*scrm-8*) genes. 300 ng of RNA were converted to cDNA using a High-Capacity RNA-to-cDNA kit™ (Applied Biosystems) and RNA was cleaned with DNase I for 15 minutes prior to cDNA conversion (Qiagen, Chatsworth, CA). qRT-PCR reactions were carried out in 10 µL volumes using TaqMan Fast Advanced master mix, TaqMan gene expression arrays for each gene (Table S2), and 1:19 diluted in water cDNA. All gene probes spanned exons and StepOne Plus system (Applied Biosystems) was used for all amplifications with a program of 10 min at 95 °C, followed by 40 cycles of 10 s at 95 °C and 30 s at 60 °C. Negative controls and minus reverse transcription (−RT) negative controls were run for every gene/sample to check for DNA contamination.

*Dissolution Experiments*

We used reverse dialysis to determine dissolution of the exposure suspensions. Pristine and transformed ZnO MNPs were suspended in synthetic soil pore water (SSPW, test media). Two concentrations (0.75 and 7.5 mg $L^{-1}$) of Zn as pristine ZnO MNPs, phosphatized ZnO MNPs (pZnO MNPs), and sulfidized ZnO MNPs (sZnO MNPs), identical to those used for the reproduction toxicity test were prepared in triplicates by adding sonicated MNP stock suspensions to the SSPW media (pH =8.2) in a 50 mL metal-free polypropylene centrifuge tube. The tubes were vortexed and then placed in a cup horn sonicator for 45 mins at 100% power. 0.8 mL of SSPW media (with no added Zn) were loaded into Pur-A-Lyzer™ Midi dialysis cells (3.5 kDa molecular weight cutoff, Sigma-Aldrich) and the cells were then placed in 50 mL polypropylene tubes containing a 45 mL of 0.75 or 7.5 mg $L^{-1}$ of as-synthesized and transformed ZnO MNPs, $ZnSO_4$ (*i.e.* an ion control treatment), or a no Zn added control (*i.e.* the SSPW media with no Zn). The tubes were tightly closed and agitated on an orbital shaker at 150 rpm under darkness at 20

°C. After a 24 hour of equilibration, the samples were taken from each of the dialysis cells (the dissolved fraction) and acidified to 0.15 M $HNO_3$. For measurement of the total Zn (dissolved + particles), samples were taken from the solution outside of the dialysis cell at 0 hr and after 24 hr of equilibration, brought to 0.75 M $HNO_3$, heated to 100˚C in a microwave digestion system for 10 min, and then diluted to 0.15 M $HNO_3$. The Zn concentration was measured by inductively coupled plasma mass spectrometry (ICP-MS) (Agilent 7500 cx, Santa Clara, CA). The speciation of Zn at thermodynamic equilibrium in SSPW media was modeled using Visual MINTEQ, version 3.0.

*Zn speciation*

To determine the speciation of Zn in nematode tissues, we performed synchrotron-based X-ray micro-spectroscopy. To generate complete Longitudinal Sections (LS) nematodes needed to be embedded for cryo-sectioning perpendicular to the cutting surface. To achieve this, a layer of OCT was introduced to cover the base of the cryo-mold and solidified using a dry-ice isopropanol bath. A layer of OCT mixed with fresh nematodes was subsequently introduced into the cryomold which was then inserted (horizontally) into the top of a 50 ml falcon and after gentle centrifugation, the OCT was again solidified using a dry-ice isopropanol bath. The block thus generated was sectioned at 10 µm and sections air dried prior to mounting on metal free polyimide film (Kapton) for synchrotron analysis and graphite discs for analytical SEM. Micro-spectroscopy was performed on beamline X26A, National Synchrotron Light Source, Brookhaven National Laboratory, Upton, NY, USA. The distribution of Zn was mapped by scanning the sections in an X-ray beam with an approximate spot size of 7 x 7 µm and an incident energy set at 10,500 eV. The Zn $K_{\alpha 1}$ emission (8638.9 eV) was detected using a silicon drift detector (Vortex ME4, Hitachi). An ion chamber immediately upstream of the K-B mirror enclosure was used to normalize for incident beam

intensity. We performed spectral fitting to extract the fluorescence intensity due to the Zn $K_{\alpha 1}$ emission. Data were plotted and quantified using ImageJ (https://imagej.nih.gov/ij/). Several areas of sufficient Zn fluorescence intensity from each section were further analyzed by performing X-ray absorption near edge spectroscopy (XANES). Spectral normalization, background subtraction, and linear combination fitting were performed using Athena to determine Zn speciation(Ravel and Newville 2005).

*Statistical Analysis*

Analysis of Variance (ANOVA) with post-hoc Dunnett's multiple comparison corrections were applied to test whether each concentration within a treatment was significantly different from control for mortality and reproduction experiments. Homogeneity of variance and normality of errors assumptions were checked using Q-Q plots and studentized residual plots. $EC_{30}$ and, when appropriate, $EC_{50}$ values were calculated from parameters determined using linear regression. SAS v9.4 (SAS Institute, Cary, NC, USA) was used for all statistical analyses and SigmaPlot 12.3 (Systat, San Jose, CA, USA) was used to generate mortality and reproduction figures.

## Results and Discussion

*Toxicities of pristine and transformed ZnO-MNPs*

In all tested treatments and concentrations, *C. elegans* mortality did not exceed 30%. Reproduction was the most sensitive endpoint, with decreases observed of up to 80% (Figs. 1 and 2). Mortality and reproduction responses were similar for both ZnO-MNPs and $ZnSO_4$. For reproduction, the $EC_{50}$ values for $ZnSO_4$ and ZnO-MNPs were 1.23 (95% CI 1.03-1.42) mg Zn $L^{-1}$ and 1.19 (95% CI 0.92-1.46) mg Zn $L^{-1}$, respectively (Table S3). The similarity in *C. elegans* responses to pristine ZnO-MNPs and $Zn^{2+}$ has been observed previously (Ma, Bertsch et al. 2009). However, the $EC_{50}$ values in our study are about 10-fold less than those reported by Ma et al.,

while being similar to those reported by Gupta et al., 2015(Yin, Cheng et al. 2011, Gupta, Kushwah et al. 2015). $LC_{50}$ values ranging from 300 µg Zn $L^{-1}$ to more than 1.0 g Zn $L^{-1}$ have been reported for pristine ZnO (Khare, Sonane et al. 2011, Yin, Cheng et al. 2011, Gupta, Kushwah et al. 2015). This variation is likely due to the difference in media chosen for the exposures (SSPW in this study versus K-medium and K-medium with sodium acetate buffer added in the Ma et al. and Gupta et al. respectively, studies). The different developmental stages at which the tests were conducted (L3 in this study versus 3 and 4-days old adults in the Ma et al and Gupta et al., respectively, studies) could have also contributed to the variability in the $LC_{50}$ values.

Toxicity, defined as a significantly different response from control, was substantially decreased when *C. elegans* were exposed to either of the transformed ZnO-MNPs as compared to pristine ZnO-MNPs (Figs. 1 and 2). For both endpoints, a 10-fold higher concentration was necessary to achieve similar levels of toxicity when comparing results from either $ZnSO_4$ or pristine ZnO-MNPs to the transformed pZnO- and sZnO-MNPs. The $EC_{50}$ values were very similar between both transformed pZnO- and sZnO-MNPs, 11.57 (95% CI 9.65 - 13.49) mg Zn $L^{-1}$ and 11.29 (9.25 - 13.34) mg Zn $L^{-1}$, respectively (Table S3; Fig. 2). Similar trends were also observed in our previous study (Starnes, Unrine et al. 2015) of sulfidized Ag-MNPs. However, in contrast with this study, the toxicity of $Ag^+$ was about 10-fold greater than that of the pristine Ag-MNPs (Starnes, Unrine et al. 2015). In that study the highest percentage of dissolution for pristine Ag-MNPs at lowest concentration of 0.05 did not exceed 6% (Starnes, Unrine et al. 2015), while dissolution of pristine ZnO-MNPs in this study is 66% at lowest concentration of 0.75 mg $L^{-1}$ tested. Thus, these differences in toxicity for Ag-MNPs or nearly identical responses for ZnO-MNPs between pristine MNPs and their respective ions are likely due to the lower solubility of Ag-MNPs relative to ZnO-MNPs.

360 The observed decrease in toxicity between transformed and pristine ZnO-MNPs is also
361 consistent with our dissolution data, where the transformed ZnO-MNPs demonstrated lower levels
362 of dissolution than pristine ZnO-MNPs (Fig. 3). All ZnO-MNPs showed concentration-dependent
363 dissolution, with percent dissolved Zn being greater at 0.75 mg Zn $L^{-1}$ than 7.5 mg Zn $L^{-1}$
364 concentrations (Fig. 3). As expected, pristine ZnO-MNPs had the highest percent dissolved Zn at
365 both concentrations (66% at 0.75 mg Zn $L^{-1}$ and 12% at 7.5 mg Zn $L^{-1}$). Additionally, both
366 transformed ZnO MNP treatments had significantly lower dissolved Zn than pristine ZnO MNPs
367 at both concentrations. Among the transformed ZnO-MNPs, the percent dissolved Zn were similar
368 (about 6%) at 7.5 mg Zn $L^{-1}$, while it was significantly higher for pZnO-MNPs at 0.75 mg $L^{-1}$ Zn
369 (49.1% for pZnO- and 15.7% for sZnO-MNPs). The greater dissolution at low concentration of
370 pZnO- compared to sZnO- is unexpected because $Zn_3(PO_4)_2$ has a Ksp value (in pure water) of
371 $10^{-33}$ compared to a Ksp of $10^{-25}$ for ZnS (Dean 1985). However, the protocol we used for
372 phosphatation results in 51% residual ZnO while the sulfidation protocol results in nearly complete
373 sulfidation(Ma, Levard et al. 2013, Rathnayake, Unrine et al. 2014). It is important to note that the
374 solubility measurements were taken without presence of bacteria and nematodes and therefore the
375 dissolution observed in the actual experiments with the bacteria/nematodes may be different. We
376 analyzed dissolution without nematodes present because ions released from the NPs could bind to
377 nematode tissues and would not be recovered during centrifugation, therefore underestimating
378 dissolution.

379 According to the dissolution data, pristine ZnO-MNPs are almost completely dissolved at
380 both tested concentrations. This, taken together with the mortality and reproduction results, (Figs.
381 1 and 2) suggest that a large portion of the observed toxicity from pristine ZnO-MNPs is likely
382 due to released $Zn^{2+}$. However, the data from the particle free supernatant versus whole solution

experiment demonstrate that mortalities for the nematodes exposed to particle free supernatants of ZnO-, pZnO-, and sZnO-MNPs showed nearly a threefold decrease compared to whole solutions, and were not significantly different from that in controls. Mortalities in the whole suspensions were 17% for ZnO-MNPs, 18% for pZnO-MNPs, and 19% for sZnO-MNPs (Fig. S7). When nematodes were exposed to supernatants of $ZnSO_4$, the mortality was 21%, similar to the 20% mortality observed in the whole (un-centrifuged) $ZnSO_4$ solution. This indicates that although the toxicity of $ZnSO_4$ and ZnO-MNPs are similar, the toxicity of ZnO-, pZnO- and sZnO-MNPs are not entirely due to the release of dissolved Zn into exposure solution. This does not rule out release of dissolved Zn in vivo, however.

The x-ray fluorescence intensity and Zn speciation data for the nematodes exposed to pristine ZnO- and pZnO-MNPs showed that no ZnO or $Zn_3(PO_4)_2$ was present inside of the nematodes after the exposure (Fig. S8). We were unable to collect data for the animals exposed to sZnO-MNPs due to limitations on beamline availability. The best model fit suggested that Zn was complexed with sulfhydryl and carbonyl groups. Since there was no $Zn_3(PO4)_2$ or ZnO detected in the nematodes exposed to pristine or transformed pZnO-MNPs, this further indicates that the observed toxicity must be due to ions released prior and/or after their uptake. Since the dissolution rate of transformed ZnO- is lower than pristine ZnO-MNPs, it may take a longer time for them to dissolve after uptake. If the main route of uptake of the intact particles is through the *C. elegans*' gut, and environment with an average pH of 3.92 (Chauhan, Orsi et al. 2013), it is expected that all three forms of ZnO-MNPs will be eventually dissolved.

*Differentially expressed genes*

Whole genome microarray screening for all treatments resulted in 1161 genes that were significantly differentially expressed relative to control. Out of these genes, 96 were shared by all

treatments (8.3%) (Fig. 4). Among those, there were up-regulated genes associated with response to metal ions (Tvermoes, Boyd et al. 2010, Zeitoun-Ghandour, Charnock et al. 2010), such as nuclear localized metal responsive gene (*numr-1*) and both metallothionein genes (*mtl-1, mtl-2*). The upregulation of *numr-1* by all Zn treatments was independently confirmed with qRT-PCR (Fig. S9). In previous study with Ag-MNPs, *numr-1* responded to Ag- ions and Ag-MNPs but not sulfidized Ag-MNPs (Starnes D. 2016). In this study both pristine and transformed ZnO-MNPs upregulated expression of *numr-1* indicating on the effects due to dissolution. Metallothioneins are small cysteine-rich proteins involved in metal detoxification and maintenance of physiological Zn (Zeitoun-Ghandour, Charnock et al. 2010). There are two isoforms of metallothionein in *C. elegans* and both genes responded to all Zn treatments. Out of 193 genes responding to $ZnSO_4$, only 49 genes were unique to $ZnSO_4$, the remaining 144 genes were shared among all treatments (Figure 4). Taken together with the dissolution and toxicity data, this further suggests that the effects in all treatments are partially attributed to the release of $Zn^{2+}$ ions, either in the exposure media or in vivo. When comparing transcriptomic responses between pristine and transformed ZnO-MNP treatments, the stronger similarity (66% shared genes) was observed between ZnO-MNP and sZnO-MNPs while the responses between ZnO-MNPs and pZnO-MNPs had less commonality (40% shared genes). Exposure to pZnO-NPs resulted in the highest number of differentially expressed genes (992) with 512 of these being unique. Exposure to ZnO-MNPs and sZnO-MNPs resulted only in 31(out of 455) and 78 (out of 453), respectively, unique genes further emphasizing distinctiveness in the responses to the transformed pZnO-MNPs.

When hierarchical cluster analysis was performed, all replicates clustered together within their respective treatments. We also observed that all three MNP treatments grouped closer together than with $ZnSO_4$ (Fig. 5). If the toxicity of MNP treatments had been only due to the

429 release of $Zn^{2+}$, we would expect a random distribution of the replicates rather than ordering into
430 two major groups. There have been a limited number of published toxicogenomic studies on the
431 effects of the metal or metal oxide MNPs in invertebrates (Starnes D. 2016), (Roh, Sim et al. 2009,
432 Tsyusko, Unrine et al. 2012, Poynton, Lazorchak et al. 2013, Rocheleau, Arbour et al. 2015,
433 Gomes, Roca et al. 2018). In a toxicogenomic study with pristine ZnO-MNPs in the benthic
434 amphipod *Hyalella azteca,* a random distribution of the ZnO-MNP and $Zn^{2+}$ replicates was
435 observed after hierarchical clustering. This indicates that transcriptomic responses were similar
436 between ions and pristine MNPs, despite ZnO-MNPs being more toxic to *H. azteca* (Poynton,
437 Lazorchak et al. 2013). The authors suggested that the higher toxicity of the particles might be due
438 to enhanced uptake of $Zn^{2+}$ from the MNP treatment(Poynton, Lazorchak et al. 2013). In our
439 previous study on the toxicogenomic effects of both transformed and pristine Ag-MNPs in *C.*
440 *elegans,* the replicates also grouped within their treatments. However, more commonality in
441 response was observed between $Ag^{+}$ and pristine Ag-MNPs than between $Ag^{+}$ and sulfidized sAg-
442 MNPs or between pristine Ag-MNPs and sAg-MNPs (Starnes D. 2016).

443 *qRT-PCR confirmation*

444 The mRNA levels for four genes (*numr-1*, *pgp-5*, *pgp-6* and *scrm-8*) selected from both
445 the shared and unique pools were confirmed independently with qRT-PCR (Fig. S9). The roles of
446 *numr-1* is desribed in the text above, when discussing the shared genes among all treatments. The
447 involvement of *pgp-5* in the shared ABC transporter pathway is discussed below. The *pgp-6*,
448 similarly to *pgp-5*, is related to P-glycoproteins in the ATP-binding cassette transporters . These
449 gene is predicated to be important for the exporting of exogenous toxins and was up-regulated by
450 all Zn treatments (Zhao, Sheps et al. 2004, Kurz, Shapira et al. 2007). The fourth gene, scramblase
451 (*scrm-8*), which was up-regulated in all ZnO-MNP but not $ZnSO_4$ treatments, is responsible for

maintaining phospholipid asymmetry and signaling events in apoptosis in *C. elegans.* It is homologous to phospholipid scramblase 1 (*plscr-1*), which is highly conserved in mammals (Wang, Wang et al. 2007).

*Shared and Unique Biological Pathways*

Using pathway analysis in Partek, DAVID and Pathview we identified pathways that were significant for at least one treatment. Only three pathways (Aminoacyl-tRNA biosynthesis, Lysosome and ABC transporters) were shared by multiple treatments. No pathways were common to all treatments (Table 1). Interestingly, the Aminoacyl-tRNA biosynthesis pathway was shared by all MNP treatments but not $ZnSO_4$. The number of genes that were up-regulated in this pathways vary from 49 to 54 (the list of the genes is provided in a SI Table S). While the main function of the aminoacyl-tRNAs is in protein synthesis, their role has been also demonstrated in gene expression, cell wall formation, labeling of proteins for degradation, and antibiotic biogenesis(Raina and Ibba 2014). The increase in the cleaved tRNA fragments has been also shown to occur in *C. elegans* during aging (Kato, Chen et al. 2011). The ABC transporter pathway was shared by both pristine ZnO- and phosphatized pZnO-MNPs, while the lysosome pathway was shared among the $ZnSO_4$ and both transformed pZnO- and sZnO-MNP treatments. The ABC transporter pathway has been shown to be associated with metal detoxification(Martinez-Finley and Aschner 2011). Among the up-regulated genes of this pathway were *haf-7 and pgp-5*. The expression of *pgp-5* has been confirmed by qRT-PCR (Fig. S9). The *pgp-5* is related to P-glycoproteins in the ATP-binding cassette transporters and its role has been shown to play a role in response to bacterial stimulus and heavy metals (*pgp-5*) (Zhao, Sheps et al. 2004, Kurz, Shapira et al. 2007).

It is interesting that the lysosome pathway was identified during pathway analysis for both transformed ZnO-MNPs and $ZnSO_4$. As the lysosome pathway has been implicated previously in our toxicogenomic study of *C. elegans* exposed to Ag-MNPs, it is reasonable to suggest that the acidic environment in these vesicles could be involved in the dissolution of MNPs after cellular uptake by endocytosis (Starnes D. 2016). In another study with Au-MPs, significantly up-regulated genes were calpains, which are associated with calpain-cathepsine mechanism leading to lysosome rupture (Tsyusko, Unrine et al. 2012). However, lysosomes also serve other functions, such as digestion of cellular debris and autophagy. A possible explanation is that apoptosis or other cellular damage caused by the $ZnSO_4$ and ZnO-MNP treatments resulted in an increased demand for digestion of cellular components. The two transformed ZnO-MNP treatments were found to share only a single pathway (lysosome), and pristine ZnO-MNPs and phosphatized pZnO-MNPs only share a single pathway (ABC transporters). This suggests that there is some commonality in the response to pristine and transformed ZnO-MNPs by *C. elegans*.

Among unique pathways affected by the exposures there were 13 related to the pZnO-MNP treatment. The FoxO signaling pathway, which has been associated with oxidative stress, was one of this pathways. Previous study demonstrated that ZnO-MNPs are capable of generating reactive oxygen species in sufficient quantities to cause toxicity in *C. elegans* (Yin, Cheng et al. 2011). However, in our study pZnO-MNPs caused down-regulation of the genes in this pathway, including the ones encoding antioxidant enzymes, superoxide dismutase (*sod-3*) and catalase (*ctl-3*) genes. This suggests that the observed response of the genes from this pathway to pZnO-MNP exposure is not associated with oxidative stress. Other unique pathways induced by pZnO-MNPs included pathways associated with amino acid synthesis and metabolism (*cel00270, cel00410, cel00380,cel00280*), which are linked to both longevity and general stress responses in *C. elegans*

(Pietsch, Saul et al. 2012). Metabolic pathways (*cel00500, cel00640*) have been thoroughly examined in relationship to the control of lifespan and aging of the nematodes (Finkel and Holbrook 2000, Murphy, McCarroll et al. 2003, Hertweck, Göbel et al. 2004). Combined with a limited number of pathways shared with the other treatments, it is difficult to attribute all of the observed effects of pZnO-MNPs to toxicity due to Zn ions. The larger size of pZnO-MNPs compared to pristine and sZnO-MNPs could cause mechanical damage of the *C. elegans* intestinal wall and can explain why the pathways linked to digestion and metabolism are affected by this treatment. Differences in levels of proteins and oxidative damage of proteins associated with digestion and metabolism were also observed in our previous study of $CeO_2$-MNP toxicity in *C. elegans* and were suggestive of damage to intestinal epithelia (Arndt, Oostveen et al. 2017). The additional unique pathways identified in the pZnO-MNP treatment as well as the lack of shared pathways between pristine ZnO- and sZnO-MNPs supports the hypothesis that transformed ZnO-MNPs have some distinct effects that are independent of their pristine starting materials.

*Shared and Unique Gene Ontologies*

Gene ontologies (GO) reveal a total of 89 Biological Processes (BP), 28 Molecular Function (MF), and 10 Cellular Compartment (CC) terms (Tables S4-S6). Each identified term had to meet a *p*-value cut off ($p<0.05$) and have at least 3 genes associated with that GO term. Complete tables with GO ids, genes in category, *p*-values, and fold enrichment can be found in the SI (Tables S4 - S6). In BP terms, the majority of the overlap occurred with terms relating to defense, response, and stress. MF terms came from cuticle related terms. In CC, the only overlapping term was for collagen trimmer. These overlapping terms represent 13% of the returned terms, with 87% of the terms being specific to MNP treatments. There were a total of eight BP terms shared among all treatments. These included defense response, immune response, innate

immune response, response to bacterium, response to external stimulus, response to stimulus, response to inorganic substance, and response to stress. Shared BPs indicate that both ions and all MNP treatments caused stress in *C. elegans*. Interestingly, several of the responses (responses to bacterium, innate immunity) are similar to ones observed when *C. elegans* are exposed to pathogenic bacteria. The indication of the response to metal ions was also found among such BPs as "response to cadmium ion" shared among ions, pristine ZnO- and phosphatized pZnO-MNPs, and "response to metal ion" shared among ions and both transformed MNPs. MFs shared by all treatments included two GOs, "structural constituent of cuticle" and "structural molecule activity", both of which include genes related to cuticle function. Similarly, activation of many genes associated with cuticle structure was previously observed in response to sulfidized Ag-MNPs but not ions (Starnes D. 2016). The only CC GO term shared by all treatments in this study was "collagen trimer", which is also associated with *C. elegans* cuticle. Trimerization domains of collagens are necessary for proper collagen folding into triple helix and mutations in these domains in collagens are associated with connective tissue diseases in humans (Boudko, Engel et al. 2012). There were thirteen BP, three MF, and one CC that were shared between $ZnSO_4$ and at least one other MNP treatment. Only four GO terms (2 BP, 2 MF) were shared by ZnO-MNPs and at least one of the transformed ZnO-MNPs. The transformed ZnO-MNPs shared of total 15 BP terms between them, including several terms related to defense response and innate immunity as well as response to metal ions.

Exposure to the transformed pZnO-MNPs resulted in the highest number of unique GOs (18 out of 45 in BP, 6 out of 16 MF, and 4 out of 6 CC) compared to exposure to other treatments. Among these GOs, most were BPs related to reproduction, e.g., spermatogenesis, meiotic cell cycle, and germ-line sex determination. Exposure to sZnO-MNPs resulted in seven unique BP and

two unique MF terms. Exposure to sZnO-MNPs returned two BP terms related to sulfur metabolism, while the MF terms where related to carbohydrate binding and hydrolase activity, and no CC terms. The number of unique GOs observed for the transformed MNPs suggests that *C. elegans* responded differentially to pristine and transformed ZnO-MNPs. One of the CC terms for pZnO-MNPs was related to P granules, which are germ granules with the role in totipotency to prevent germ cell transformation into somatic cells(Updike, Knutson et al. 2014). The two core genes of the P granules, *pgl-1* and *glh-1*, along with the other two genes (*pgl-2* and *glh-3*) associated with this GO were significantly down-regulated in response to the pZnO-MNPs. Depletion of the core components of the P-granules has been shown to induce expression of neuronal and muscle markers in the germ cells and adversely affect reproduction in *C. elegans* (Updike, Knutson et al. 2014). The ten unique pathways induced in response to phosphatized pZnO-MNPs as well as the high number of unique GO Terms in both transformed treatments suggest that the responses to pZnO and sZnO-MNPs are distinct from those to the pristine ZnO-MNPs and cannot be explained fully by the release of dissolved Zn.

*Conclusions*

The near identical responses in mortality and reproduction endpoints of the nematodes exposed to pristine ZnO-MNPs and $ZnSO_4$indicate that a significant part of the toxicity of pristine ZnO-MNPs is likely due to dissolution. The nearly a ten-fold decrease in the toxicity for the same endpoints observed after pristine ZnO-MNPs were transformed in the presence of either phosphate or sulfide, is consistent with reductions in toxicity observed for transformed sulfidized Ag-MNPs. Both pZnO-MNPs and sZnO-MNPs represent major transformation products expected to be present in biosolids that are applied to agricultural fields, indicating that the wastewater treatment process will decrease the initial toxicity of ZnO-MNPs in this exposure

scenario. Microarray data and pathway analysis showed that there are distinct responses to MNP exposures and $ZnSO_4$ exposure. However, all MNP treatments induced responses of the three genes associated with metal ion toxicity and 50% of the genes responding to $ZnSO_4$ were shared among all forms of ZnO-MNP treatments. This suggests that release of $Zn^{2+}$, either in exposure media or in vivo, played a role in toxicity of not only pristine but all forms of Zn-MNPs. Comparisons of transcriptomic responses between pristine and transformed Zn-MNP treatments reveal higher similarity in responses between ZnO-MNPs and sZnO-MNPs than ZnO-MNPs with pZnO-MNPs. The 13 unique biological pathways identified in pZnO-MNP treatment indicate distinct toxicity mechanism for this transformed ZnO-MNPs. Taken together our results from toxicity and the biological pathway and GO analyses indicate that the role of the dissolved $Zn^{2+}$ in the *C. elegans* toxicity was much greater after exposure to the pristine rather than transformed ZnO-MNPs.

## Acknowledgements

We acknowledge the assistance of D. Wall, D. Arndt, S. Shrestha, A. Wamucho, and Y. Thompson. *Caenorhabditis elegans* strains were provided by the Caenorhabditis Genetics Center, which is funded by the NIH Office of Research Infrastructure Programs (P40 OD010440). Funding for this research was provided by the United States Environmental Protection Agency (U.S. EPA) Science to Achieve Results Grant RD 834574. JU and OT are supported by the U.S. EPA and National Science Foundation (NSF) through cooperative agreement EF-0830093, Center for Environmental Implications of Nanotechnology (CEINT). SL was partially funded by the Tracy Farmer Institute for Sustainability and the Environment. Portions of this work were performed at Beamline X26A, National Synchrotron Light Source (NSLS), Brookhaven National Laboratory. X26A is supported by the Department of Energy (DOE) - Geosciences (DE-FG02-92ER14244 to The University of

Chicago - CARS). Use of the NSLS was supported by DOE under Contract No. DE-AC02-98CH10886. Any opinions, findings, conclusions, or recommendations expressed in this material are those of the author(s) and do not necessarily reflect the views of the EPA or NSF. This work has not been subjected to EPA or NSF review, and no official endorsement should be inferred.

**Table 1.** Pathways identified by Partek, DAVID and Pathview using lists of significantly differentially expressed genes after *Caenorhabditis elegans* were exposed for 48 hours to $ZnSO_4$, pristine Zinc Oxide manufactured nanoparticles (ZnO-MNPs), phosphatized (pZnO-MNPs), or sulfidized (sZnO-MNPs) in synthetic soil pore water. The fold enrichment and p-values are estimated from Partek. The number in parenthesis in "Genes in Pathway" column are additional genes that according to DAVID or Pathview analysis are also included in the pathways. The upregulated and down-regulated genes in pathways are shown in red and blue font, respectively.

| KEGG ID | Pathway Name | Genes in Pathway | Fold Enrichment | P-Value | Treatment |
|---|---|---|---|---|---|
| **cel02010** | ABC transporters[P,D] (*haf-7, pgp-5, pgp-1*) | 2 (3) | 6.231 (9.9) | 0.002 (0.003) | ZnO |
| **cel00970** | *Aminoacyl-tRNA biosynthesis[D, PW] | 49 (50) | 2.6 | 1.1E-16<br>1.5E-25 | ZnO |
| **cel04142** | Lysosome (*cpr-3*, *W07B8.4*) | 2 | 3.574 | 0.028 | ZnSO4 |
| **cel00270** | Cysteine and Methionine metabolism[P, D] (*cysl-2*, *sams-5*, *metr-1*, *spds-1*, *got-2.1*, *cth-1*) | 4 (6) | 5.739 (4.4) | 0.003<br>(0.0046) | pZnO |
| **cel02010** | ABC transporters[P, D, PW] (*haf-7*, *pgp-1*, *pgp-5*, *pgp-11*, *pgp-4*) | 3 (5) | 5.233 (8.6) | 0.005<br>(0.00018)<br>(0.00041) | pZnO |
| **cel00410** | beta-Alanine metabolism[P, D] (*F09F7.4*, *ech-6*, *spds-1*) | 3 | 4.664 (4.3) | 0.009 (0.03) | pZnO |
| **cel00500** | Starch and sucrose metabolism[P] (*aagr-1*, *ugt-46*) | 3 | 4.347 | 0.013 | pZnO |
| **cel04142** | Lysosome[P, D] (*asah-1*, *cpr-3*, *nuc-1*, *haf-7*, *asm-3*, *gba-4*) | 5 (6) | 4.344 (2.7) | 0.013 (0.02) | pZnO |
| **cel00380** | Tryptophan metabolism[P] (*ctl-3*, *ech-9*, *ech-6*) | 3 | 4.203 | 0.015 | pZnO |
| **cel01200** | Carbon metabolism[P, D] (*F09F7.4*, *acs-19*, *cysl-2*, *ctl-3*, *ech-6*, *F26H9.5*, *sdha-2*) | 5 (7) | 3.850 (2.9) | 0.021<br>(0.0051) | pZnO |
| **cel00640** | Propanoate metabolism[P,D] (*F09F7.4*, *acs-19*, *ech-6*) | 3 | 3.818 (3.7) | 0.022 (0.044) | pZnO |

| | | | | | |
|---|---|---|---|---|---|
| **cel04068** | FoxO signaling pathway[P] (*ctl-3*, *plk-2*, *plk-3*, *sod-3*) | 4 | 3.731 | 0.024 | pZnO |
| **cel01230** | Biosynthesis of amino acids [P, D] (*cysl-2*, *sams-5*, *metr-1*, *F26H9.5*, *got-2.1*, *cth-1*, *gln-5*, *gln-6*) | 4 (8) | 3.503 (2.9) | 0.030 (0.02) | pZnO |
| **cel00280** | Valine, leucine an isoleucine degradation[P] (*F09F7.4*, *ech-9*, *ech-6*) | 3 | 3.489 | 0.031 | pZnO |
| **cel00970** | *Aminoacyl-tRNA biosynthesis[D,PW] | 53 | 1.5 | 0.00064 (2.75E-12) | pZnO |
| **cel04320** | Dorso-ventral axis formation[D, PW] (*cpb-1*, *cpb-3*, *fog-1*, *prg-2*) | 4 | 7.3 | 0.0017 (0.0031) | pZnO |
| **cel00250** | Alanine, aspartate and glutamate metabolism[D] | 5 | 4.6 | 0.004 | pZnO |
| **cel00910** | Nitrogen metabolism[D] (*bca-1*, *gln-5*, *gln-6*) | 3 | 6.9 | 0.0083 | pZnO |
| **cel00220** | Arginine biosynthesis [D] (*got-2.1*, *gln-5*, *gln-6*) | 3 | 5.9 | 0.013 | pZnO |
| **cel04142** | Lysosome[P] (*cpr-3*, *asm-3*) | 2 | 3.574 | 0.028 | sZnO |
| | *Aminoacyl-tRNA biosynthesis[D, PW] | 47 | 2.6 | 8.8E-16 1.45E-23 | sZnO |

599 *The list of genes upregulated in Aminoacyl t-RNA biosynthesis pathways is provided in SI (Table S7)

## Figure Legends

**Figure 1**. Mortality of L3 *Caenorhabditis elegans* without feeding after 24 hours of exposure to $ZnSO_4$, pristine (ZnO-MNPs), phosphatized (pZnO-MNPs), or sulfidized (sZnO-MNPs) zinc oxide manufactured nanoparticles in synthetic soil pore water. Data are presented as mean percent mortality with error bars indicating standard error of the mean. An asterisk (*) indicates significantly different than control at $\alpha = 0.05$ based on Dunnett's test. The control treatment is represented by a concentration of 0.

**Figure 2.** Mean total number of offspring per adult nematode *Caenorhabditis elegans* after 48 hours exposure to $ZnSO_4$, pristine (ZnO-MNPs), phosphatized (pZnO-MNPs), or sulfidized (sZnO-MNPs) zinc oxide manufactured nanoparticles in synthetic soil pore water in the presence of bacterial food (*Escherichia coli* strain OP50). An asterisk (*) indicates significantly different than control at $\alpha = 0.05$ based on Dunnett's test.

**Figure 3**. The percent dissolution of ZnSO4 (ion control treatment), pristine, phosphatized (pZnO-MNPs), and sulfidized (sZnO-MNPs) zinc oxide manufactured nanoparticles in synthetic soil pore water (SSPW) adjusted to pH 8.2 over 24 h. (A) 0.75 mg $kg^{-1}$; (B) 7.5 mg $kg^{-}1$. Data are means ± S.D., $n = 3$ replicates. The Zn concentrations in control were below the instrument detection limits and are not shown.

**Figure 4.** Venn diagram of the significantly up/down regulated genes with a p-value $\leq 0.05$ and fold change of ± 2.0. *Caenorhabditis elegans* were exposed for 48 hours to $ZnSO_4$, pristine (ZnO-MNPs), phosphatized (pZnO-MNPs) and sulfidized (sZnO-MNPs) zinc oxide manufactured nanoparticles in synthetic soil pore water.

**Figure 5**. Hierarchical clustering histogram of differentially expressed genes from *Caenorhabditis elegans* exposed for 48 hours to $ZnSO_4$, pristine (ZnO-MNPs), phosphatized (pZnO-MNPs), and sulfidized (sZnO-MNPs) zinc oxide manufactured nanoparticles in synthetic soil pore water.

## References


Arndt, D. A., E. K. Oostveen, J. Triplett, D. Allan Butterfield, O. V. Tsyusko, B. Collin, D. L. Starnes, J. Cai, J. B. Klein, R. Nass and J. M. Unrine (2017). "The role of charge in the toxicity of polymer-coated cerium oxide nanomaterials to *Caenorhabditis elegans*." Comparative Biochemistry and Physiology Part C: Toxicology & Pharmacology **201**: 1-10.

Boudko, S. P., J. Engel and H. P. Bächinger (2012). "The crucial role of trimerization domains in collagen folding." The International Journal of Biochemistry & Cell Biology **44**(1): 21-32.

Chauhan, V. M., G. Orsi, A. Brown, D. I. Pritchard and J. W. Aylott (2013). "Mapping the pharyngeal and intestinal pH of *Caenorhabditis elegans* and real-time luminal pH oscillations using extended dynamic range pH-sensitive nanosensors." ACS Nano **7**(6): 5577-5587.

Chen, C., J. M. Unrine, J. D. Judy, R. W. Lewis, J. Guo, D. H. McNear and O. V. Tsyusko (2015). "Toxicogenomic responses of the model legume *Medicago truncatula* to aged biosolids containing a mixture of nanomaterials ($TiO_2$, Ag, and ZnO) from a pilot wastewater treatment plant." Environmental Science & Technology **49**(14): 8759-8768.

Dean, J. A. (1985). "Lange's handbook of chemistry."

EPA (1995). A Guide to the Biosolids Risk Assessments for the EPA. Washington, D.C.

Finkel, T. and N. J. Holbrook (2000). "Oxidants, oxidative stress and the biology of ageing." Nature **408**(6809): 239-247.

Gomes, S. I. L., C. P. Roca, N. Pegoraro, T. Trindade, J. J. Scott-Fordsmand and M. J. B. Amorim (2018). "High-throughput tool to discriminate effects of NMs (Cu-NPs, Cu-nanowires, CuNO3, and Cu salt aged): transcriptomics in Enchytraeus crypticus." Nanotoxicology **12**(4): 325-340.

Gottschalk, F., T. Sonderer, R. W. Scholz and B. Nowack (2009). "Modeled environmental concentrations of engineered nanomaterials ($TiO_2$, ZnO, Ag, CNT, Fullerenes) for different regions." Environmental Science & Technology **43**(24): 9216-9222.

Gupta, S., T. Kushwah, A. Vishwakarma and S. Yadav (2015). "Optimization of ZnO-NPs to investigate their safe application by assessing their effect on soil nematode *Caenorhabditis elegans*." Nanoscale Research Letters **10**(1): 1-9.

Hertweck, M., C. Göbel and R. Baumeister (2004). "C. elegans SGK-1 is the critical component in the Akt/PKB kinase complex to control stress response and life span." Developmental cell **6**(4): 577-588.

Huang da, W., B. T. Sherman and R. A. Lempicki (2009). "Bioinformatics enrichment tools: paths toward the comprehensive functional analysis of large gene lists." Nucleic Acids Res **37**(1): 1-13.

Huang da, W., B. T. Sherman and R. A. Lempicki (2009). "Systematic and integrative analysis of large gene lists using DAVID bioinformatics resources." Nat Protoc **4**(1): 44-57.

Irizarry, R. A., B. Hobbs, F. Collin, Y. D. Beazer-Barclay, K. J. Antonellis, U. Scherf and T. P. Speed (2003). "Exploration, normalization, and summaries of high density oligonucleotide array probe level data." Biostatistics **4**(2): 249-264.

Ju-Nam, Y. and J. R. Lead (2008). "Manufactured nanoparticles: An overview of their chemistry, interactions and potential environmental implications." Science of The Total Environment **400**(1–3): 396-414.

Judy, J. D., D. H. McNear, C. Chen, R. W. Lewis, O. V. Tsyusko, P. M. Bertsch, W. Rao, J. Stegemeier, G. V. Lowry, S. P. McGrath, M. Durenkamp and J. M. Unrine (2015). "Nanomaterials in biosolids inhibit nodulation, shift microbial community composition, and result in increased metal uptake relative to bulk/dissolved metals." Environmental Science & Technology **49**(14): 8751-8758.

Kato, M., X. Chen, S. Inukai, H. Zhao and F. J. Slack (2011). "Age-associated changes in expression of small, noncoding RNAs, including microRNAs, in C. elegans." RNA (New York, N.Y.) **17**(10): 1804-1820.

Khare, P., M. Sonane, R. Pandey, S. Ali, K. C. Gupta and A. Satish (2011). "Adverse effects of $TiO_2$ and ZnO nanoparticles in soil nematode, *Caenorhabditis elegans*." Journal of Biomedical Nanotechnology **7**(1): 116-117.

Kurz, C. L., M. Shapira, K. Chen, D. L. Baillie and M.-W. Tan (2007). "*Caenorhabditis elegans pgp-5* is involved in resistance to bacterial infection and heavy metal and its regulation requires TIR-1 and a p38 map kinase cascade." Biochemical and Biophysical Research Communications **363**(2): 438-443.

Lahive, E., M. Matzke, M. Durenkamp, A. J. Lawlor, S. A. Thacker, M. G. Pereira, D. J. Spurgeon, J. M. Unrine, C. Svendsen and S. Lofts (2017). "Sewage sludge treated with metal nanomaterials inhibits earthworm reproduction more strongly than sludge treated with metals in bulk/salt forms." Environmental Science: Nano **4**(1): 78-88.

Landa, P., R. Vankova, J. Andrlova, J. Hodek, P. Marsik, H. Storchova, J. C. White and T. Vanek (2012). "Nanoparticle-specific changes in *Arabidopsis thaliana* gene expression after exposure to ZnO, $TiO_2$, and fullerene soot." Journal of Hazardous Materials **241-242**: 55-62.

Levard, C., E. M. Hotze, B. P. Colman, A. L. Dale, L. Truong, X. Y. Yang, A. J. Bone, G. E. Brown, Jr., R. L. Tanguay, R. T. Di Giulio, E. S. Bernhardt, J. N. Meyer, M. R. Wiesner and G. V. Lowry (2013). "Sulfidation of silver nanoparticles: natural antidote to their toxicity." Environ Sci Technol **47**(23): 13440-13448.

Levard, C., X. Yang, J. N. Meyer and G. V. Lowry (2014). "Response to comment on “Sulfidation of silver nanoparticles: natural antidote to their toxicity”." Environmental Science & Technology **48**(10): 6051-6052.

Lombi, E., E. Donner, E. Tavakkoli, T. W. Turney, R. Naidu, B. W. Miller and K. G. Scheckel (2012). "Fate of Zinc Oxide nanoparticles during anaerobic digestion of wastewater and post-treatment processing of sewage sludge." Environmental Science & Technology **46**(16): 9089-9096.

Lucid, J. D., O. Fenton and M. G. Healy (2013). "Estimation of maximum biosolids and meat and bone meal application to a low P index soil and a method to test for nutrient and metal losses." Water, Air, & Soil Pollution **224**(4): 1-12.

Luo, W., G. Pant, Y. K. Bhavnasi, J. S. G. Blanchard and C. Brouwer (2017). "Pathview Web: user friendly pathway visualization and data integration." Nucleic Acids Research **45**(W1): W501-W508.

Ma, H., P. M. Bertsch, T. C. Glenn, N. J. Kabengi and P. L. Williams (2009). "Toxicity of manufactured zinc oxide nanoparticles in the nematode *Caenorhabditis elegans*." Environmental Toxicology and Chemistry **28**(6): 1324-1330.

Ma, R., C. Levard, J. D. Judy, J. M. Unrine, M. Durenkamp, B. Martin, B. Jefferson and G. V. Lowry (2014). "Fate of Zinc Oxide and Silver nanoparticles in a pilot wastewater treatment plant and in processed biosolids." Environmental Science & Technology **48**(1): 104-112.

Ma, R., C. Levard, F. M. Michel, G. E. Brown Jr and G. V. Lowry (2013). "Sulfidation mechanism for zinc oxide nanoparticles and the effect of sulfidation on their solubility." Environmental science & technology **47**(6): 2527-2534.

Martinez-Finley, E. J. and M. Aschner (2011). "Revelations from the nematode *Caenorhabditis elegans* on the complex interplay of metal toxicological mechanisms." Journal of Toxicology **2011**: 10.

Martínez, C. E., K. A. Bazilevskaya and A. Lanzirotti (2006). "Zinc coordination to multiple ligand atoms in organic-rich surface soils." Environmental Science & Technology **40**(18): 5688-5695.

Mueller, N. C. and B. Nowack (2008). "Exposure modeling of engineered nanoparticles in the environment." Environmental Science & Technology **42**(12): 4447-4453.

Murphy, C. T., S. A. McCarroll, C. I. Bargmann, A. Fraser, R. S. Kamath, J. Ahringer, H. Li and C. Kenyon (2003). "Genes that act downstream of DAF-16 to influence the lifespan of *Caenorhabditis elegans*." Nature **424**(6946): 277-283.

Mwaanga P., M. S., Shumbula P., and Nyirenda J. (2017). "Investigating the toxicity of Cu, CuO and ZnO nanoparticles on earthworms in urban soils." Journal of Pollution Effects & Control **5**(3): 1000195.

Pietsch, K., N. Saul, S. C. Swain, R. Menzel, C. E. W. Steinberg and S. R. Stürzenbaum (2012). "Meta-analysis of global transcriptomics suggests that conserved genetic pathways are responsible for quercetin and tannic acid mediated longevity in *C. elegans*." Frontiers in Genetics **3**: 48.

Poynton, H. C., J. M. Lazorchak, C. A. Impellitteri, B. Blalock, M. E. Smith, K. Struewing, J. Unrine and D. Roose (2013). "Toxicity and transcriptomic analysis in *Hyalella azteca* suggests increased exposure and susceptibility of epibenthic organisms to Zinc Oxide nanoparticles." Environmental Science & Technology **47**(16): 9453-9460.

Raina, M. and M. Ibba (2014). "tRNAs as regulators of biological processes." Frontiers in Genetics **5**(171).

Rathnayake, S., J. M. Unrine, J. Judy, A.-F. Miller, W. Rao and P. M. Bertsch (2014). "Multitechnique investigation of the pH dependence of phosphate induced transformations of ZnO nanoparticles." Environmental science & technology **48**(9): 4757-4764.

Ravel, B. and M. Newville (2005). "ATHENA, ARTEMIS, HEPHAESTUS: data analysis for X-ray absorption spectroscopy using IFEFFIT." Journal of Synchrotron Radiation **12**(4): 537-541.

Rocheleau, S., M. Arbour, M. Elias, G. I. Sunahara and L. Masson (2015). "Toxicogenomic effects of nano- and bulk-$TiO_2$ particles in the soil nematode *Caenorhabditis elegans*." Nanotoxicology **9**(4): 502-512.

Roh, J. Y., S. J. Sim, J. Yi, K. Park, K. H. Chung, D. Y. Ryu and J. Choi (2009). "Ecotoxicity of silver nanoparticles on the soil nematode *Caenorhabditis elegans* using functional ecotoxicogenomics." Environ Sci Technol **43**(10): 3933-3940.

Romero-Freire, A., S. Lofts, F. J. Martín Peinado and C. A. M. van Gestel (2017). "Effects of aging and soil properties on zinc oxide nanoparticle availability and its ecotoxicological effects to the earthworm *Eisenia andrei*." Environmental Toxicology and Chemistry **36**(1): 137-146.

Spisni, E., S. Seo, S. H. Joo and C. Su (2016). Release and toxicity comparison between industrial- and sunscreen-derived nano-ZnO particles.

Starnes D., L., S., Unrine, J., Starnes, C., Oostveen, E., Lowry, G., Bertsch, P., and Tsyusko, O. (2016). "Distinct transcriptomic responses of *Caenorhabditis elegans* to pristine and sulfidized silver nanoparticles. ." Journal of Environmental Pollution ***In Press***.

Starnes, D. L., J. M. Unrine, C. P. Starnes, B. E. Collin, E. K. Oostveen, R. Ma, G. V. Lowry, P. M. Bertsch and O. V. Tsyusko (2015). "Impact of sulfidation on the bioavailability and toxicity of silver nanoparticles to *Caenorhabditis elegans.*" Environmental Pollution **196**(0): 239-246.

Tsyusko, O. V., J. M. Unrine, D. Spurgeon, E. Blalock, D. Starnes, M. Tseng, G. Joice and P. M. Bertsch (2012). "Toxicogenomic responses of the model organism *Caenorhabditis elegans* to gold nanoparticles." Environ Sci Technol **46**(7): 4115-4124.

Tvermoes, B. E., W. A. Boyd and J. H. Freedman (2010). "Molecular characterization of numr-1 and numr-2: genes that increase both resistance to metal-induced stress and lifespan in *Caenorhabditis elegans*." Journal of Cell Science **123**(12): 2124-2134.

763 Tyne, W., S. Lofts, D. J. Spurgeon, K. Jurkschat and C. Svendsen (2013). "A new medium for
764 *Caenorhabditis elegans* toxicology and nanotoxicology studies designed to better reflect natural
765 soil solution conditions." Environ Toxicol Chem **32**(8): 1711-1717.
766 Updike, D. L., A. K. a. Knutson, T. A. Egelhofer, A. C. Campbell and S. Strome (2014). "Germ-
767 granule components prevent somatic development in the *C. elegans* germline." Current biology :
768 CB **24**(9): 970-975.
769 Vance, M. E., T. Kuiken, E. P. Vejerano, S. P. McGinnis, M. F. Hochella, D. Rejeski and M. S. Hull
770 (2015). "Nanotechnology in the real world: Redeveloping the nanomaterial consumer products
771 inventory." Beilstein Journal of Nanotechnology **6**: 1769-1780.
772 Wang, H., R. L. Wick and B. Xing (2009). "Toxicity of nanoparticulate and bulk ZnO, $Al_2O_3$ and
773 $TiO_2$ to the nematode *Caenorhabditis elegans*." Environmental Pollution **157**(4): 1171-1177.
774 Wang, X., J. Wang, K. Gengyo-Ando, L. Gu, C.-L. Sun, C. Yang, Y. Shi, T. Kobayashi, Y. Shi, S.
775 Mitani, X.-S. Xie and D. Xue (2007). "C. elegans mitochondrial factor WAH-1 promotes
776 phosphatidylserine externalization in apoptotic cells through phospholipid scramblase SCRM-1."
777 Nat Cell Biol **9**(5): 541-549.
778 Williams, P. L. and D. B. Dusenbery (1988). "Using the nematode *Caenorhabditis elegans* to
779 predict mammalian acute lethality to metallic salts." Toxicology and Industrial Health **4**(4): 469-
780 478.
781 Xiaoshan, Z., W. Jiangxin, Z. Xuezhi, C. Yung and C. Yongsheng (2009). "The impact of ZnO
782 nanoparticle aggregates on the embryonic development of zebrafish ( Danio rerio )."
783 Nanotechnology **20**(19): 195103.
784 Xiu, Z. M., Q. B. Zhang, H. L. Puppala, V. L. Colvin and P. J. Alvarez (2012). "Negligible particle-
785 specific antibacterial activity of silver nanoparticles." Nano Lett **12**(8): 4271-4275.
786 Yin, L., Y. Cheng, B. Espinasse, B. P. Colman, M. Auffan, M. Wiesner, J. Rose, J. Liu and E. S.
787 Bernhardt (2011). "More than the ions: the effects of silver nanoparticles on *Lolium*
788 *multiflorum*." Environ Sci Technol **45**(6): 2360-2367.
789 Zeitoun-Ghandour, S., J. M. Charnock, M. E. Hodson, O. I. Leszczyszyn, C. A. Blindauer and S. R.
790 Stürzenbaum (2010). "The two *Caenorhabditis elegans* metallothioneins (CeMT-1 and CeMT-2)
791 discriminate between essential zinc and toxic cadmium." FEBS Journal **277**(11): 2531-2542.
792 Zhao, Z., J. A. Sheps, V. Ling, L. L. Fang and D. L. Baillie (2004). "Expression analysis of ABC
793 transporters reveals differential functions of tandemly duplicated genes in *Caenorhabditis*
794 *elegans*." Journal of Molecular Biology **344**(2): 409-417.
795 Zhong Lin, W. (2004). "Zinc oxide nanostructures: growth, properties and applications." Journal
796 of Physics: Condensed Matter **16**(25): R829.

797

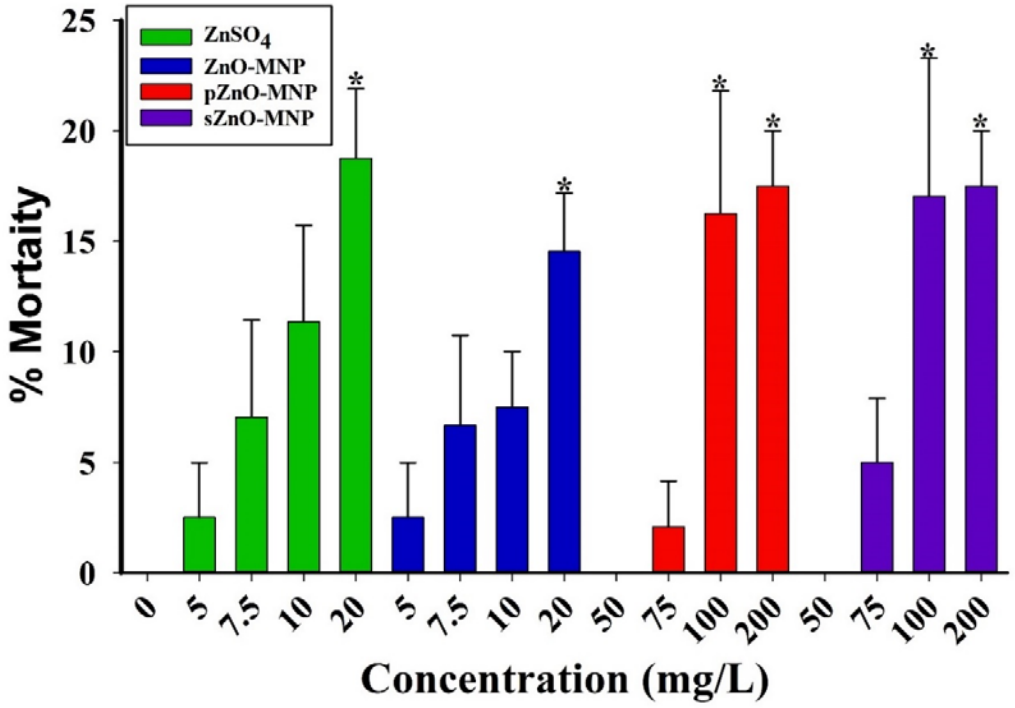


Figure 1. Mortality of L3 *Caenorhabditis elegans* without feeding, after 24 hours of exposure to $ZnSO_4$, pristine (ZnO-MNPs), phosphatized (pZnO-MNPs), or sulfidized (sZnO-MNPs) zinc oxide manufactured nanoparticles in synthetic soil pore water. Data are presented as mean percent mortality with error bars indicating standard error of the mean. An asterisk (*) indicates significantly different than control at $\alpha = 0.05$ based on Student's t-test.

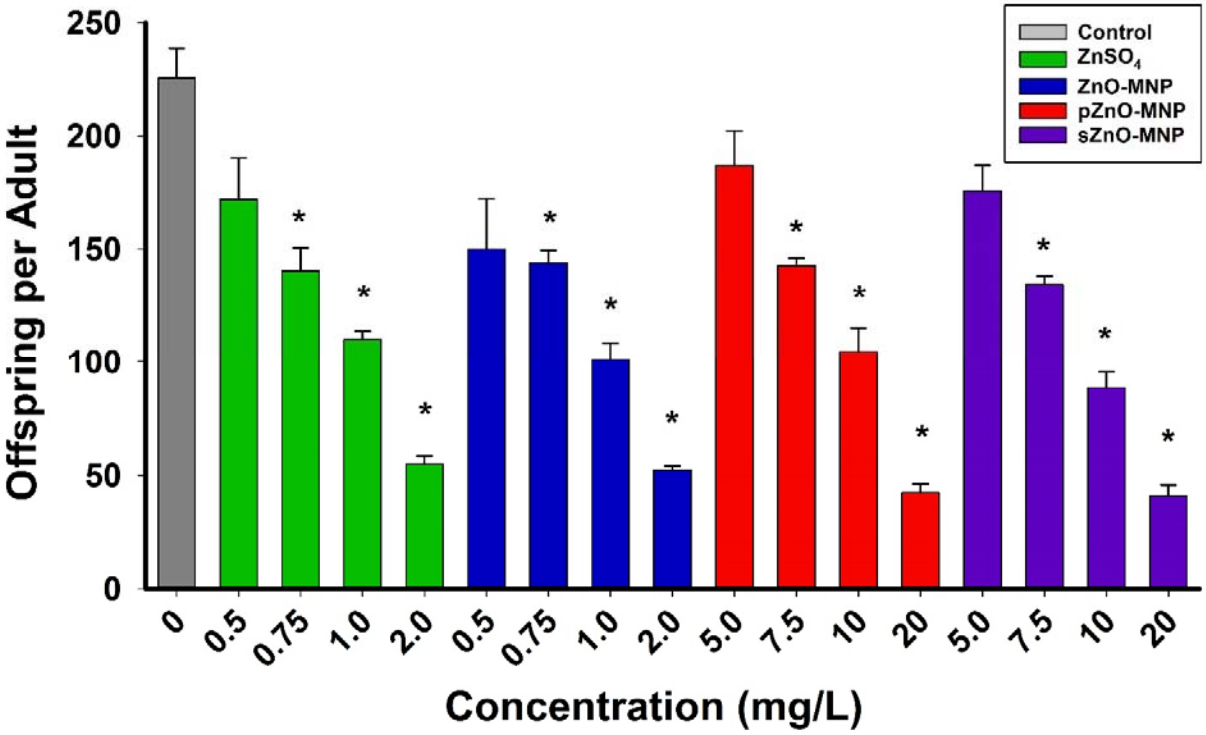


Figure 2. Mean total number of offspring per adult nematode *Caenorhabditis elegans* after 48 hours exposure to $ZnSO_4$, pristine (ZnO-MNPs), phosphatized (pZnO-MNPs), or sulfidized (sZnO-MNPs) zinc oxide manufactured nanoparticles in synthetic soil pore water in the presence of bacterial food (*Escherichia coli* strain OP50). An asterisk (*) indicates significantly different than control at $\alpha = 0.05$ based on Student's t-test.

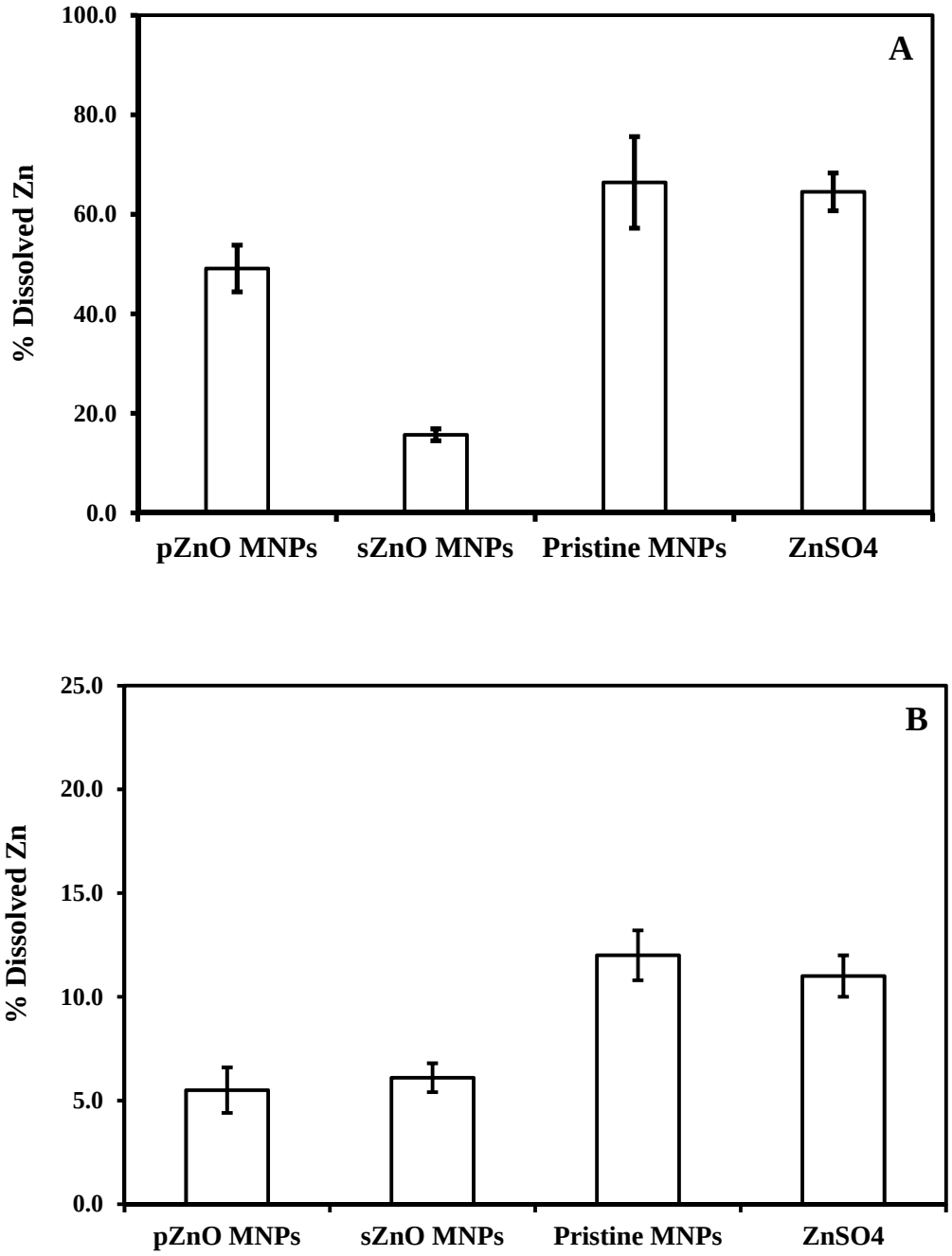


Figure 3. The percent dissolution of $ZnSO_4$ (ion control treatment), pristine, phosphatized (pZnO-MNPs), and sulfidized (sZnO-MNPs) zinc oxide manufactured nanoparticles in synthetic soil pore water adjusted to pH 8.2 over 24 h. (A) 0.75 mg $L^{-1}$; (B) 7.5 mg $L^{-1}$. Data are means ± S.D., $n = 3$ replicates. The Zn concentrations in control were below the instrument detection limits and are not shown.

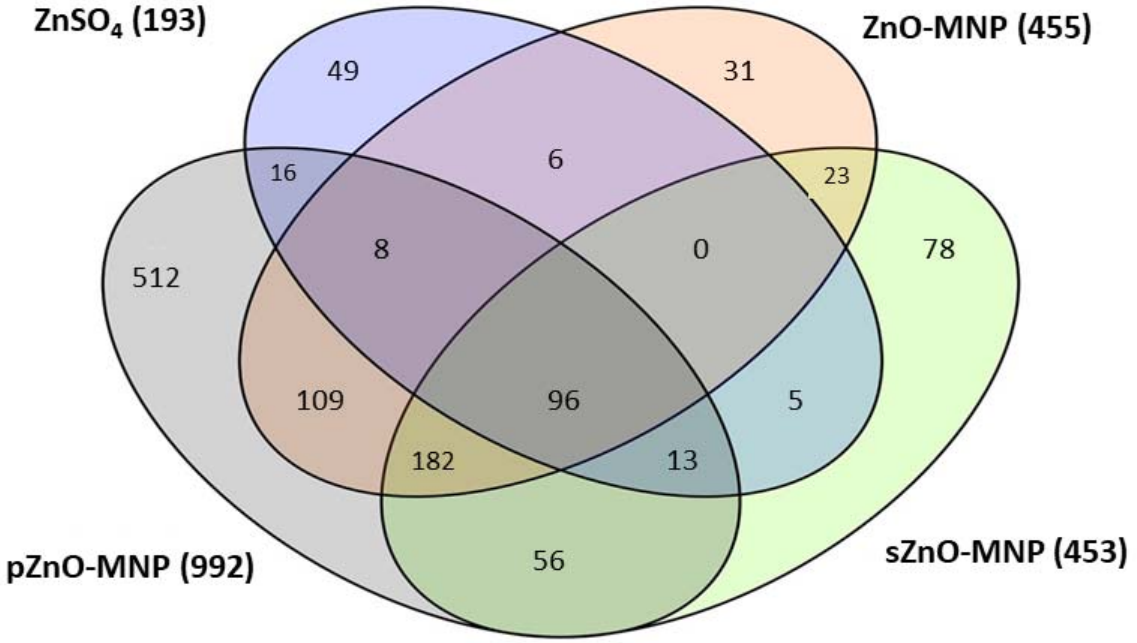


Figure 4. Venn diagram of the significantly up/down regulated genes ($p \leq 0.05$ and fold change ± 2) of . *Caenorhabditis elegans* were exposed for 48 hours to $ZnSO_4$, pristine (ZnO-MNPs), phosphatized (pZnO-MNPs) and sulfidized (sZnO-MNPs) zinc oxide manufactured nanoparticles in synthetic soil pore water.

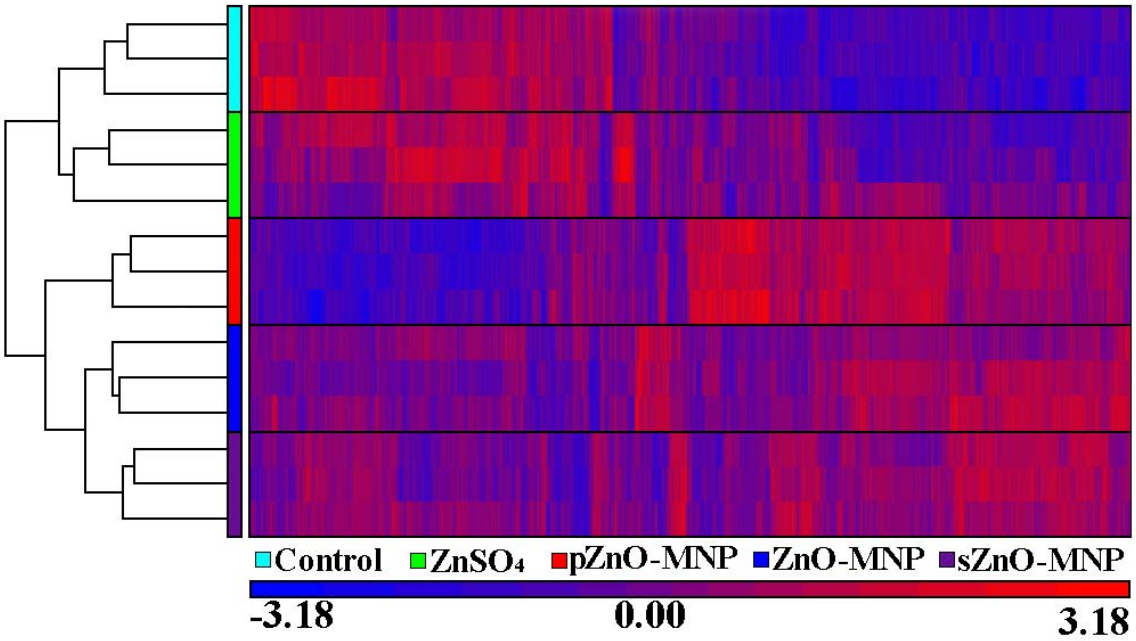


Figure 5. Hierarchical clustering histogram of differentially expressed genes from *Caenorhabditis elegans* exposed for 48 hours to $ZnSO_4$, pristine (ZnO-MNPs), phosphatized (pZnO-MNPs), and sulfidized (sZnO-MNPs) zinc oxide manufactured nanoparticles in synthetic soil pore water.